# Project 4 FYS4150

Vilde Mari Reinertsen

November 19, 2017

**Abstract**

In this project we used many different methods to model a two dimensional lattice using the Ising model. These methods were Monte Carlo sampling, the Metropolis algorithm, parallelizing and random number generators. Monte Caro methods can be used in many different and complicated physical problems. The Metropolis algorithm gives an easy shortcut because we only need a function that is proportional to the probability distribution function, we do not need to calculate the partition function.

We started with a small two dimensional lattice at one temperature, then increased the lattice size and calculated properties of a magnetic material for a temperature interval. We used the temperature dependence of the properties to evaluate the critical temperature and the second order phase transition.

The program used in this project can be found at GitHub.

# Contents

# 1 Introduction

The aim of this project is to use a model of a magnetic material to explore different new aspects of programming. Among them are random number generators, the Monte Carlo method, the Metropolis algorithm and parallelizing. These are all important tools when programming physical systems.

We want to simulate a two dimensional ferromagnetic material using the Ising model. We are using Monte Carlo sampling with the Metropolis algorithm to find the steady state of the system at different temperatures.We will calculate the mean values of important properties of a magnetic material, the energy, the magnetic moment, the susceptibility and the heat capacity. Finally, we will use the results at different temperatures to find the critical temperature where the material has a phase transition from ferromagnetic with a spontaneous magnetic moment, to a paramagnet with zero magnetic moment.

This report contains some theory on the Ising model, statistics and properties of a magnetic material. It explains the methods used in the calculation and simulation. Furthermore, the results are presented together with a discussion of the result. Finally some concluding remarks are presented.

# 2 Theory

The theory and method sections are based mainly on chapter 5, 11, 12 and 13 in Computational Physics [1].

## 2.1 Ising model

The two dimensional Ising model is a statistical model that allows us to investigate the temperature dependence of different properties of a magnet. Our model consists of a two dimensional lattice of spins that can be in two different states, spin up, $\uparrow$, or spin down, $\downarrow$ [2]. The number of spins in each dimension is $L$ and the lattice is assumed to be quadratic. In our system we do not have an applied field, $B_a = 0$. The energy of our system is then given by Equation 1.

$$E = -J \sum_{\langle kl \rangle}^{N} s_k s_l \tag{1}$$

where in our system $J > 0$, $J$ is the coupling constant, giving a ferromagnetic ordering, and $s_k$, $s_l = \pm 1$, $s_k$ is the $k$-th spin of $N$ number of spins.

To get easier numbers to do calculations with we scaled $e^{-\beta E}$ by setting $T' = \frac{k_B T}{J}$ and $E' = JE_{kl}$, with $E_{kl} = \sum_{<k,l>} s_k s_l$ Then $e^{-\beta E}$ can be written as $e^{-E'/T'}$.

## 2.2 Periodic boundary conditions

Because we did not have an infinite lattice, we included periodic boundary conditions. That means that when the spins on the edges are flipped, we use the spins on the other side of the lattice as nearest neighbors, to calculate the change in energy.

## 2.3 Introduction to statistics

The methods in this project require some statistics. Equation 2 shows the probability density and in the Ising model, the probability distribution function (PDF) is Boltzmann distribution (Equation 3) where $Z$ is the partition function that normalizes the probability (Equation 4). To calculate $Z$, we need to know all the different states, $i$, and their energy, $E_i$. It can be calculated for small systems (2.5 Analytical solutions for $L$=2), but it would be very time consuming to include it in Monte Carlo Sampling. A method that does not include it, is necessary.

$$P(a \leq X \leq b) = \int_b^a p(x)\, dx \tag{2}$$

$$P_i(\beta) = \frac{e^{-\beta E_i}}{Z} \tag{3}$$

$$Z = \sum_{i=1}^{M} e^{-\beta E_i} \tag{4}$$

In this project we are looking at different properties of a magnet. That is energy, magnetic moment, heat capacity and susceptibility. To get out this data form our Ising model, we need some statistical terms. We will use Monte Carlo cycles and the Metropolis algorithm to calculate the second order moment (Equation 5) and the first order moment also called the mean value (Equation 6) of the energy and the magnetic moment. These values, we can use to get the heat capacity and the susceptibility.

$$\langle x^2 \rangle = \int x^2 \, P(x) \, dx \tag{5}$$

$$\langle x \rangle = \int x \, P(x) \, dx \tag{6}$$

## 2.4 Magnetic properties

The energy of the system is found by using Equation 1. The total magnetic moment is found by adding the magnetic moments of all spins in the lattice. The susceptibility represents how a material responds to an applied magnetic field, $B_a$. The heat capacity is the ratio of heat added to a material and the resulting temperature change.

From thermodynamics we have these relations [3]:

$$\langle E \rangle = k_B T^2 \frac{\partial \ln Z}{\partial T} \qquad \langle M \rangle = k_B T \frac{\partial \ln Z}{\partial B_a}$$

$$C_V = \frac{\partial \langle E \rangle}{\partial T} \qquad \chi = \frac{\partial \langle M \rangle}{\partial B_a}$$

We are looking at the temperature dependence of these properties and finding the critical temperature, $T_C$, where the phase transition between paramagnetic and ferromagnetic occurs. When $T < T_C$ the system exhibit spontaneous magnetization, it is ferromagnetic, but when $T > T_C$ the net magnetization is zero, it is paramagnetic. This phase transition is of second order. That means that the correlation length of the system diverges when $T \to T_C$, it spans the whole system. The correlation length represents the correlation between the spins. It is a spacial unit because it indicates how far away spins can be from each other and still correlate. We can find out that the Ising model exhibits a second-order phase transition since the heat capacity diverges. The temperature dependence of the magnetic susceptibility from mean-field theory is shown in Equation 7.

$$\chi \propto (T - T_C)^{-\gamma} \tag{7}$$

where $\gamma$ is a critical exponent and is different for different materials.

The critical temperature for finite lattices is lattice dependent, the result for finite lattice sizes is related to the critical temperature for the infinite lattice by Equation 8.

$$T_C(L) - T_C(L = \infty) = aL^{-1/\nu} \tag{8}$$

## 2.5 Analytical solutions for $L$=2

Here are the calculation of the analytical values for the system where $L$=2. These were used as benchmark calculations for the numerical calculations.

Table 2.1: This table lists the possible states and their accompanying energies when $L$=2 The full list of energies without degeneration is in Table 5.1 in the Appendix.

| # ↑ | Degeneration | Energy | Magnetization |
|---|---|---|---|
| 0 | 1 | -8J | -4 |
| 1 | 4 | 0 | -2 |
| 2 | 4 | 0 | 0 |
| 2 | 2 | 8J | 0 |
| 3 | 4 | 0 | 2 |
| 4 | 1 | -8J | 4 |

First we calculated the partition function using Equation 1 and the numbers in Table 2.1:

$$Z = \sum_i^N e^{-\beta E_i} = e^{-\beta 8J} + e^{-\beta 8J} + e^{\beta 8J} + e^{\beta 8J} + 12$$

$$= 2e^{-\beta 8J} + 2e^{\beta 8J} + 12 = 4\left(\frac{e^{-\beta 8J} + e^{-\beta 8J}}{2}\right) + 12$$

$$= 4\cosh(\beta 8J) + 12$$

Using thermodynamical relations we calculate the expectation values of the energy and magnetic moment [3].

$$\langle E \rangle = k_B T^2 \left( \frac{\partial Z}{\partial T} \right)_{V,N}$$

$$= k_B T^2 \frac{\partial}{\partial T} \left[ \ln \left( 4 \cosh \left( \frac{8J}{k_B T} \right) + 12 \right) \right]$$

$$\frac{\partial \ln Z}{\partial T} = \frac{\partial Z}{\partial \beta} \frac{\partial \beta}{\partial T} = \frac{\partial \ln Z}{\partial \beta} \left( \frac{-1}{k_B T^2} \right)$$

$$\langle E \rangle = -\left( \frac{\partial Z}{\partial \beta} \right)_{V,N} = -\frac{\partial}{\partial \beta} \ln \left[ 4 \cosh \left( 8J\beta \right) + 12 \right]$$

$$= \frac{-1}{4 \cosh(8J\beta) + 12} 4 \sinh(8J\beta) 8J\beta$$

$$= \frac{-8J \sinh(8J\beta)}{3 \cosh((J\beta) + 4}$$

Following the same method, we found that:

$$\langle |M| \rangle = \frac{1}{Z} \sum_i^N M_i e^{\beta E_i} = \frac{(8J)^2 \cosh(8J\beta)}{\cosh(8J\beta) + 3}$$

$$\langle M \rangle = 0$$

$$\left\langle E^2 \right\rangle = \frac{1}{Z} \left( \sum_i^N E_i^2 e^{\beta E_i} \right) = \frac{8 \left( e^{8J\beta} + 1 \right)}{\cosh(8J\beta) + 3}$$

$$\left\langle M^2 \right\rangle = \frac{1}{Z} \left( \sum_i^N M_i^2 e^{\beta E_i} \right) = \frac{2 \left( e^{8J\beta} + 2 \right)}{\cosh(8J\beta) + 3}$$

We can use these to calculate the rest, with these definitions:

$$C_V = k\beta^2 \left( \left\langle E^2 \right\rangle - \langle E \rangle^2 \right)$$

$$\chi = \beta \left( \left\langle M^2 \right\rangle - \langle M \rangle^2 \right)$$

# 3 Method

In this project we tried out many new concepts in our algorithm.

## 3.1 Monte Carlo sampling

To reach the most likely state, the steady state, we use Monte Carlo sampling. Our Monte Carlo sampling function is given in Equation 3 and it is the Boltzmann distribution which is temperature dependent because $\beta = \frac{1}{k_b T}$. It is the probability of finding the system in state $i$. The sampling rule is explained in 3.2 Metropolis algorithm.

## 3.2 Metropolis Algorithm

We are looking at transition from one state to another. $W_{ij}$ is the transformation probability of going from state $j$ to state $i$. $\omega_i$ is our PDF, $P_i$, (Equation 3). That means that a transition from $i$ to $j$ can be written:

$$\omega_i = W_{ij} \omega_j$$

The steady state of a system can be written as:

$$\omega_i = \sum_j W_{ij} \omega_j$$

or in matrix form:

$$\hat{\omega}(t+1) = \hat{W} \hat{\omega}(t)$$

It means that our probability distribution is not changing with time (in our case Monte Carlo cycles) anymore.

In our case we do not know the transition probability, and we have to model it. We do this using the Metropolis algorithm. We separate $W_{ij}$ into two parts, the probability of accepting the move from state $j$ to state $i$, $A_{ij}$, and the probability of making the move to state $i$ when in state $j$, $T_{ij}$. We define $T_{ij}$ and $A_{ij}$ to lead the system to the most likely state.

In our case the algorithm starts with suggesting a move from state $j$ to state $i$, it does this by picking a random spin and flipping it. The picking of the spin is governed by the uniform distribution, that gives $T_{ij} = T_{ji}$, it is symmetric. The uniform distribution is baked into the random number generators.

After the move is suggested, it has to be accepted or not. This acceptance has to make the system go towards the most likely state, the steady state.

Our ratio between probabilities is:

$$\frac{A_{ij}}{A_{ji}} = \frac{\omega_i T_{ij}}{\omega_j T_{ji}} = \exp(-\beta(E_i - E_j)) = \exp(-\beta \Delta E_{ij})$$

with the Boltzmann distribution. The acceptance probability is:

$$A_{ij} = \begin{cases} \exp(-\beta \Delta E_{ij}) & \text{if } \Delta E_{ij} > 0 \\ 1 & \text{if } \Delta E_{ij} \leq 0 \end{cases} \tag{9}$$

We need to accept some moves where $\Delta E_{ij} > 0$ so that the algorithm is ergodic, that all possible states in the system can be reached, even though the probability of it happening is small.

In practice, this is how we executed the Metropolis Algorithm:

- Calculate total energy of initial lattice, $E_{tot}$.
- Calculate the possible acceptance probabilities (Equation 9) from the five possible $\Delta E$s (Table 5.2) and the temperature.
- Pick a random spin in the lattice.
- Flip the spin.
- Calculate the change in energy, $\Delta E$, from the nearest neighbors:

$$\Delta E = -J \sum_{\langle kl \rangle}^{M} s_k^2 \left(s_l^2 - s_l^1\right)$$

$$((s_l^2 - s_l^1) = -2 \text{ if } s_l^1 = 1$$
$$((s_l^2 - s_l^1) = 2 \text{ if } s_l^1 = -1$$

$$\Delta E = 2J s_l^1 \sum_{\langle k \rangle}^{M} s_k^2$$

- If $\Delta E \leq 0$ - accept new configuration.
- Update mean values:

  $E_{tot} += \Delta E$

  $M_{tot} += \Delta M = 2s_l^1$ etc.

  $\rightarrow$ Repeat
- Else if $\Delta E > 0$ - find the relevant acceptance probability, $\omega$.
- Compare $\omega$ with a random number $r \in [0, 1]$
- If $r \leq \omega$ - accept new configuration.
- Update mean values:

  $E_{tot} += \Delta E$

  $M_{tot} += \Delta M = 2s_l^1$ etc.

  $\rightarrow$ Repeat
- If $r > \omega$ - do not accept new configuration.

  $\rightarrow$ Repeat with old configuration

## 3.3 Random number generators

The random number generator (RNG) used in this project is gained from a linear congruential relation (Equation 10). Which can, with good parameters, $a$ and $c$ give a list of quasi random numbers with a maximum periodicity $M$, that means that the numbers repeat themselves after $M$ numbers. It is important that the periodicity is large compared with the number of Monte Carlo cycles, so the 'measurements' represent the truly random real world. The RNG gives a number $x_i \in [0, 1]$ because $x_i = N_i/M$. The PDF for generating random numbers in the interval $[0, 1]$ is the uniform distribution.

$$N_i = (aN_{i-1} + c)MOD(M) \tag{10}$$

## 3.4 Parallelizing

In this project we used parallelization. We used Message Passing Interface (MPI) to parallelize our code. Each process read and executes the whole program. We had to use different MPI functions to make sure that all processes sent their results to one main process that would write to file for example. Beneath is some samples of the program that shows the process.

```
int NProcesses, RankProcess;
//   MPI initializations
MPI_Init(&argc, &argv);
MPI_Comm_size(MPI_COMM_WORLD, &NProcesses);
MPI_Comm_rank(MPI_COMM_WORLD, &RankProcess);

//Sending result to RankProcess = 0
for( int i =0; i < 5; i++){
    MPI_Reduce(&meanValues[i], &
    TotalMeanValues[i], 1, MPI_DOUBLE,
    MPI_SUM, 0, MPI_COMM_WORLD);
}
```

```
if (RankProcess == 0){
    writeToFile();
}
// MPI end
MPI_Finalize();
```

## 3.5 Unit tests

In this project we did not write any unit tests, we only wrote out the results during the program development and saw if it was logical. We could have made a unit test that calculated the properties of the $L$=2-system and compared them to the analytical values calculated in the theory. This would have helped us make sure that when we made changes to the program, for example implementing parallelization and classes, the program was doing what it was supposed to do and not getting the wrong result.

Another unit test we could have included is just flipping one spin in a small matrix and checking is the change in energy is what we expect. We should use unit tests from the start in the next project.

# 4 Result and discussion

## 4.1 Compared with analytical result

We started with a small two dimensional lattice with lattice size $L$=2 and at T'= 1.0 $k_B T/J$ with random initial state. The result for energy, magnetic moment, heat capacity and susceptibility are in Figures 4.1, 4.2, 4.3 and 4.4 respectively. From the plots, we can see that the numerical result gives a good agreement with the analytical values calculated in 2.5 Analytical solutions for L=2 after approximately $5 \cdot 10^5$ Monte Carlo cycles. Table 4.1 lists the result after $10^6$ Monte Carlo cycles, and it show a good agreement as well.

Table 4.1: This table compares the analytical values for $L$=2 with the numerical ones after $10^6$ Monte Carlo cycles. The values are in units per spin and at T'=1.0 $k_B T/J$.

| | Numerical: | Analytical: |
|---|---|---|
| $\langle E \rangle$ $[E_{kl}]$ | -1.9958 | -1.9960 |
| $\langle E^2 \rangle$ $[E^2_{kl}]$ | 15.9664 | 15.9679 |
| $\langle M \rangle$ | 0.0451 | 0 |
| $\langle M^2 \rangle$ | 3.9930 | 3.9933 |
| $\langle \lvert M \rvert \rangle$ | 0.9986 | 0.9987 |
| $\chi$ $[J/k_B^T]$ | 3.9849 | 3.9933 |
| $C_V$ $[J^2/k_B^3 T^2]$ | 0.0335 | 0.0321 |

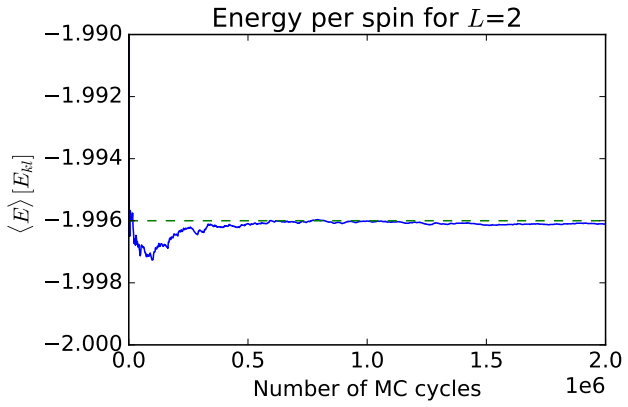


Figure 4.1: This is a plot of the expectation value of the energy per spin verus number of Monte Carlo cycles. The plot shows that we have a good agreement after $5 \cdot 10^5$ MC cycles.

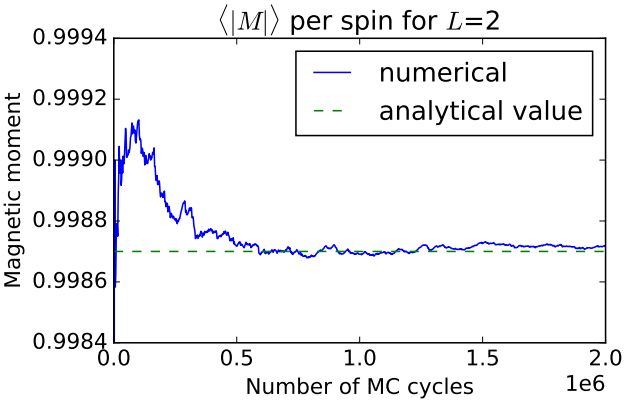


Figure 4.2: This is a plot of the expectation value of the mean absolute value of the magnetic moment per spin verus number of Monte Carlo cycles. The plot shows that we have a good agreement after $5 \cdot 10^5$ MC cycles.

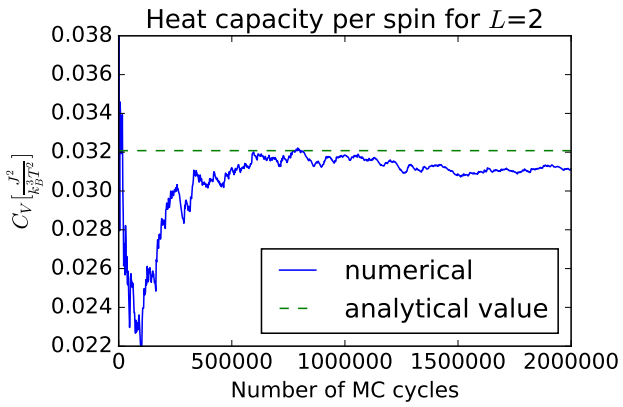


Figure 4.3: This is a plot of the heat capacity per spin verus number of Monte Carlo cycles. The plot shows that we have a good agreement after $5 \cdot 10^5$ MC cycles.

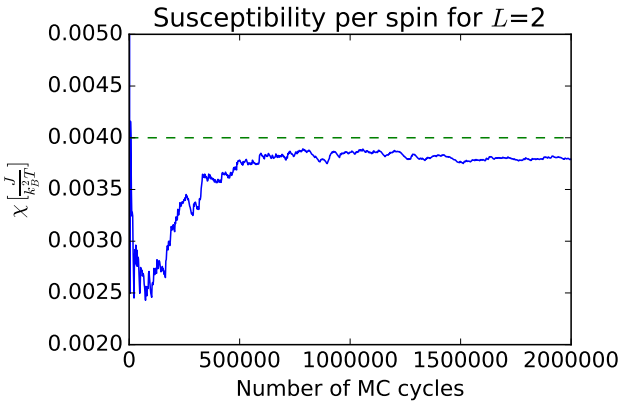


Figure 4.4: This is a plot of the susceptibility per spin verus number of Monte Carlo cycles. The plot shows that we have a good agreement after $5 \cdot 10^5$ MC cycles.

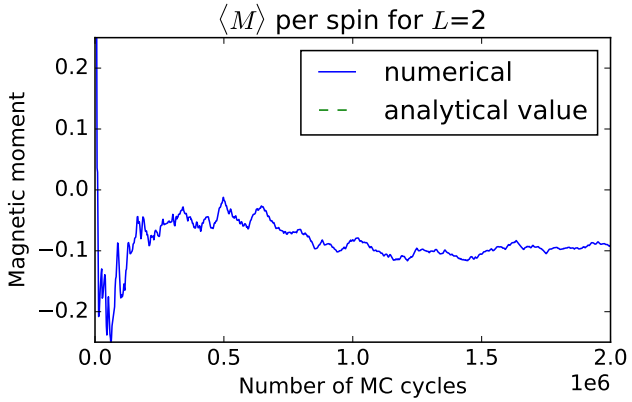


Figure 4.5: This is a plot of the expectation value of the mean value of the magnetic moment per spin verus number of Monte Carlo cycles. The plot shows that we would not have had a good agreement after $5 \cdot 10^5$ MC cycles, when not using the absolute value as in Figure 4.2.

We see that the energy converges fastest. The magnetic moment is not converging as fast but still fast, we are plotting the absolute value, and that makes it converge faster, because the oscillation between the same size, but different signs does not show. Figure 4.5 shows how the magnetic moment converges much slower. It can be shown however that the magnetic moment will converge, but slower and we would have needed more Monte Carlo cycles.

## 4.2 Equilibration time

We increased the size of the system to $L = 20$ and saw how both the temperature and the initial state affected the procedure by again plotting against number of Monte Carlo cycles.

### 4.2.1 Initial state

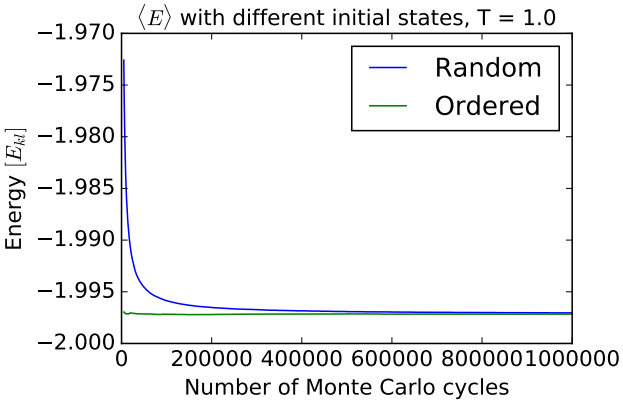


Figure 4.6: This is a plot of both the expectation value of the energy and absolute magnetic moment per spin verus number of Monte Carlo cycles at T' = 1.0 $k_B T/J$. The plot shows the difference in the behaviour of the ordered initial state and a random initial state.

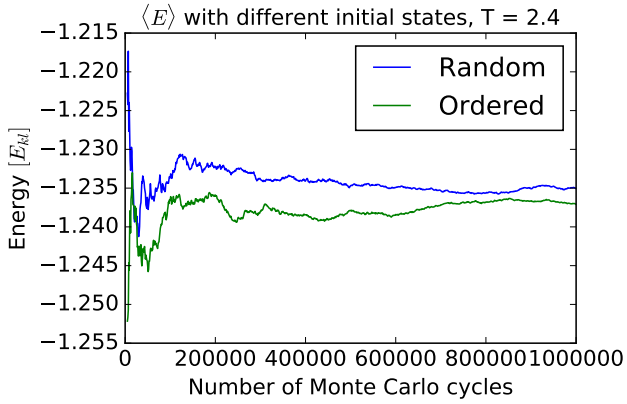


Figure 4.7: This is a plot of both the expectation value of the energy and absolute magnetic moment per spin verus number of Monte Carlo cycles at T' = 2.4 $k_B T/J$. The plot shows the difference in the behaviour of the ordered initial state and a random initial state.

Figure 4.6 compares the development of the expectation value for the energy with an ordered initial state, all spin up, and a random initial state at the temperature 1.0 $k_B T/J$. We see from the plot that the ordered initial state converges much earlier. This might be because the ordered state reflects the most likely state, better then the random state, at small temperatures.

Figure 4.7 shows the development of the expectation value for the energy with an ordered initial state and a random initial state for the temperature 2.4 $k_B T/J$. We see from the plot that the two initial states act similarly and converges similarly. They do not converge as fast as at the low temperature, but that is expected because of the increase in temperature (see 4.3 Energy probability).

Because the random initial state converged slower then the ordered one, we compared the random initial states when we looked at both the magnetic moment and the energy at the two temperatures and found an equilibrium time.

### 4.2.2 Different temperatures

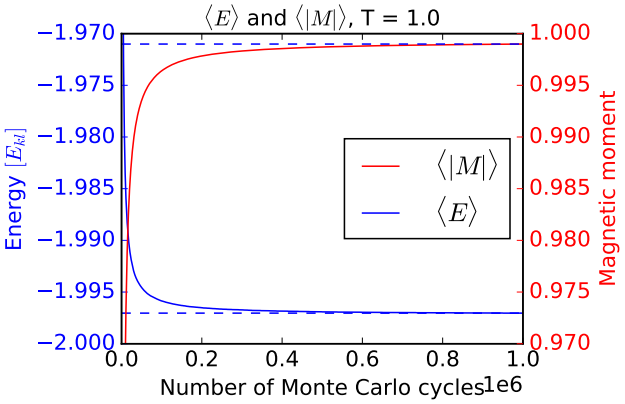


Figure 4.8: This is a plot of both the expectation value of the energy and absolute magnetic moment per spin verus number of Monte Carlo cycles at T' = 1.0 $k_B T/J$. The plot shows that an equilibrium is reached already at $2 \cdot 10^5$ MC cycles.

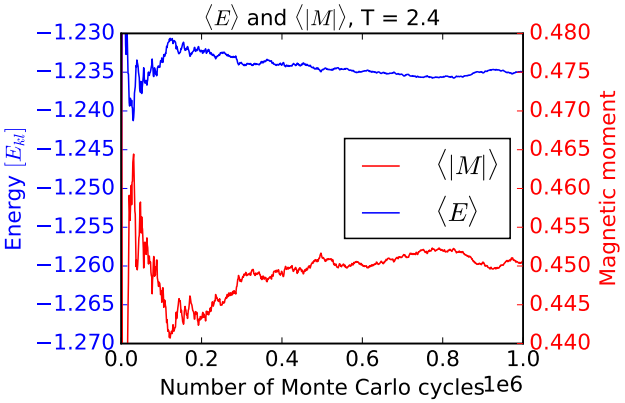


Figure 4.9: This is a plot of both the expectation value of the energy and absolute magnetic moment per spin verus number of Monte Carlo cycles at T' = 2.4 $k_B T/J$. The plot shows that an equilibrium is reached at around $5 \cdot 10^5$ MC cycles.

Figure 4.8 and Figure 4.9 shows the result for $L = 20$ at two different temperatures and give different equilibration times. Figure 4.8 shows that the values are $\pm 0.005$ from the equilibrium values already at $2 \cdot 10^5$ Monte Carlo cycles, but if we want even better accuracy, we need to wait till $5 \cdot 10^5$ Monte Carlo cycles. If we look at Figure 4.9 though, we see that the values are $\pm 0.005$ from the equilibrium values from around $5 \cdot 10^5$ Monte Carlo cycles.

The equilibration time is then approximately $5 \cdot 10^5$ Monte Carlo cycles at T' = 2.4 $k_B T/J$ and lower for the lower temperature, so $5 \cdot 10^5$ Monte

Carlo cycles is what we used when we counted the energies to get the probabilities.

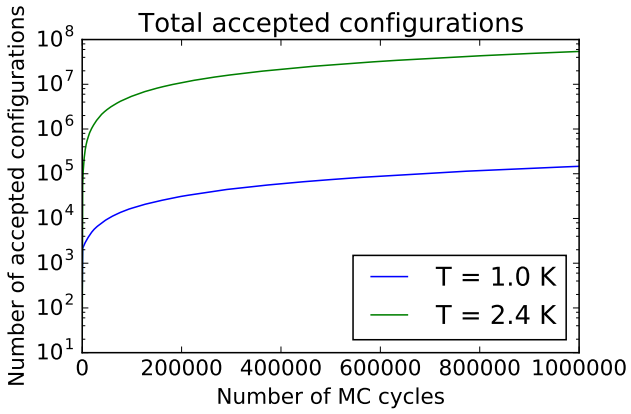


Figure 4.10: This is a plot of the total number of accepted configurations versus number of Monte Carlo cycles with random initial state.

The values are fluctuating a lot more when the temperature is higher. Figure 4.10 shows the total number of accepted configurations with increasing number of Monte Carlo cycles. It is easy to see that the algorithm accepts more configurations when the temperature is higher. It is not that easy to see, since it is a logarithmic plot, but the slope of the higher temperature one, is larger then the lower temperature one, after equilibrium. This is also what we see with the fluctuations in the expectation plots. This is what we will look into in 4.3 Energy probability.

## 4.3 Energy probability

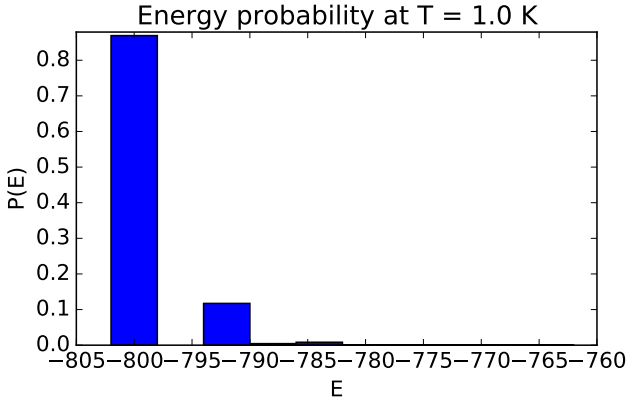


Figure 4.11: This is a plot of the energy probability when T' = 1.0 $k_B T/J$. The energy is the total energy of the 2D lattice with $20 \times 20$ spins.

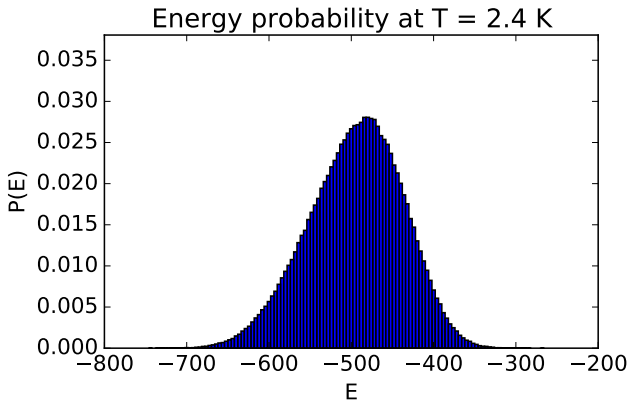


Figure 4.12: This is a plot of the energy probability when T' = 2.4 $k_B T/J$.The energy is the total energy of the 2D lattice with $20 \times 20$ spins.

Figure 4.11 shows the probability density of the energy at T' = 1.0 $k_B T/J$. It was calculated by counting the number of times an energy occurred after the equilibration time. The graph reflects the little fluctuation in the expectation values. Figure 4.12, which shows the probability density of the energy at T' = 2.4 $k_B T/J$, however, shows that with higher temperature the probability density is more smeared out around the most likely state.

This fits with the Boltzmann distribution (Equation 3). The difference in temperature changes the probability of accepting transition moves (Equation 9) 'away' from the most likely state, $\Delta E_{ij} > 0$:

$$e^{\frac{-\Delta E_{ij}}{k_B T_1}} > e^{\frac{-\Delta E_{ij}}{k_B T_2}} \qquad \text{if } T_1 > T_2$$

We calculated the variance to compare it with the probability plots in Figures 4.11 and 4.12:

The variance of the energy is given by:

$$\sigma_E^2 = \langle E^2 \rangle - \langle E \rangle^2$$

and the standard deviation is $\sigma_E = \sqrt{\sigma_E^2}$.

The connection between full width half maximum (FWHM) and standard deviation can be put as:

$$\text{FWHM} = 2\sqrt{2 \ln 2}\sigma_E \approx 2.355\sigma_E$$

for a standard distribution [4]. We will use it as a guide when comparing the graphs with the variance.

T' = 1.0 $k_B T/J$:

$$\sigma_E^2 = 638181 - (-798.855)^2 = 11.69$$

$$\sigma_E = 3.42$$

$$\text{FWHM} \approx 2.355 \cdot 3.24 = 7.63$$

It is difficult to read out a FWHM from the histogram in Figure 4.11 because of the few different energies. We might say it is around 10 if we assume it is symmetric. It fits alright with the calculated value.

T' = 2.4 $k_B T/J$:

$$\sigma_E^2 = 247886 - (-494.628)^2 = 3229.14$$

$$\sigma_E = 56.8$$

$$\text{FWHM} \approx 2.355 \cdot 56.8 = 133.76$$

It is easier to read out the FWHM from Figure 4.12. We could say it is around (560-440 =) 120, and that is around what we got.

The most important point is that the variance is much larger for larger temperatures.

## 4.4 The Critical Temperature

At last we ran the program for even bigger lattice sizes and a temperature interval, to investigate the critical temperature and the phase transition.

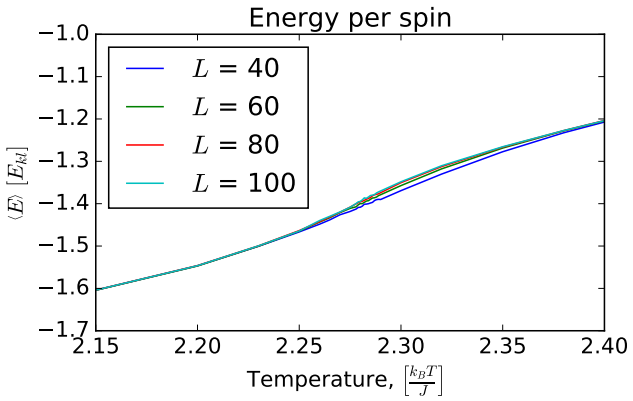


Figure 4.13: This is a plot if the energy versus temperature around the critical temperature for the different lattice sizes with $L = 40$, $L = 60$, $L = 80$ and $L = 100$.The small fluctuations are due to higher resolution in temperature around the critical temperature.

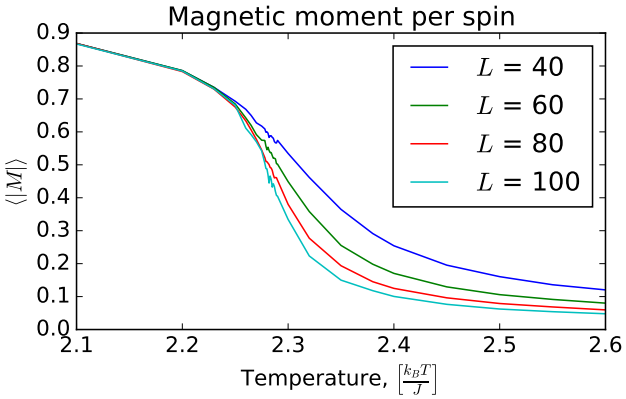


Figure 4.14: This is a plot if the absolute magnetic moment versus temperature around the critical temperature for the different lattice sizes with $L = 40$, $L = 60$, $L = 80$ and $L = 100$. The small fluctuations are due to higher resolution in temperature around the critical temperature.

Figure 4.13 shows energy as a function of temperature. We can see a change in the behavior around T' = 2.25-2.30 $k_B T/J$. This disturbance in the function might indicate a phase transition. The different sizes have the same behavior, but we can see that the slope is larger the larger the lattice, in the area of the supposed phase shift.

In Figure 4.14, which shows the temperature dependence of the absolute value of the magnetic moment, there is a clearer change around T' = 2.30 $k_B T/J$. The change is more abrupt with larger lattice sizes. The figure does indicate that we have a phase transition from a ferromagnet with magnetic moment per spin around 0.9 to a paramagnet with magnetic moment per spin around 0. We see also here that the change is more abrupt for larger lattice sizes. The tendency shows that an infinite two dimensional lattice might give an infinite steep slope at the critical temperature.

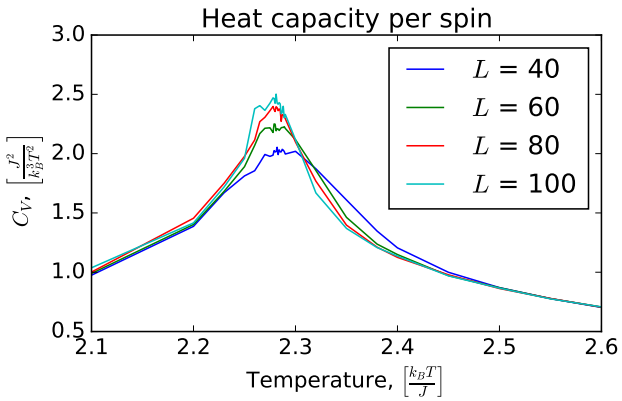


Figure 4.15: This is a plot if the heat capacity versus temperature around the critical temperature for the different lattice sizes with $L = 40$, $L = 60$, $L = 80$ and $L = 100$. The small fluctuations are due to higher resolution in temperature around the critical temperature.

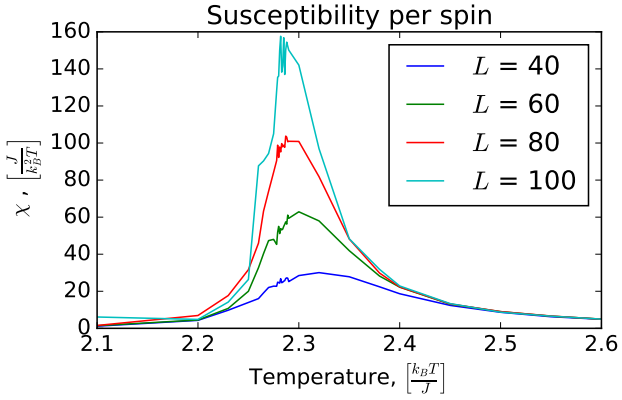


Figure 4.16: This is a plot if the susceptibility versus temperature around the critical temperature for the different lattice sizes with $L = 40$, $L = 60$, $L = 80$ and $L = 100$. The small fluctuations are due to higher resolution in temperature around the critical temperature.

Figure 4.15 shows the temperature dependency of the heat capacity. The heat capacity should diverge for a second order phase transition, due to the infinite steep slope in the energy because it is the derivative of the energy with respect to temperature. We see from the plot that the peak becomes higher when the lattice size increases, and it looks like it will diverge for an infinite big lattice.

The temperature dependency of the susceptibility shows the same tendency as the heat capacity. It should diverge as well when $T' \to T_C$ because of its inverse temperature dependency (Equation 7).

At last we used Equation 8 with $\nu = 1$ to extract $T_C(L = \infty)$. From Figure 4.15 we read out the $T_C(L)$ for $L = 40$, $L = 60$, $L = 80$ and $L = 100$. We used the result to do a linear regression for $T_C(L) = a \cdot L^{-1} + T_C(\infty)$ and find $T_C(\infty)$. The result is in Figure 4.17. $T_C(\infty)$ was found to be 2.278 $k_B T/J$. The result is not so bad compared with the exact value $T_C(\infty) = 2/\ln(1+\sqrt{2}) \approx 2.269$ $k_B T/J$ [5].

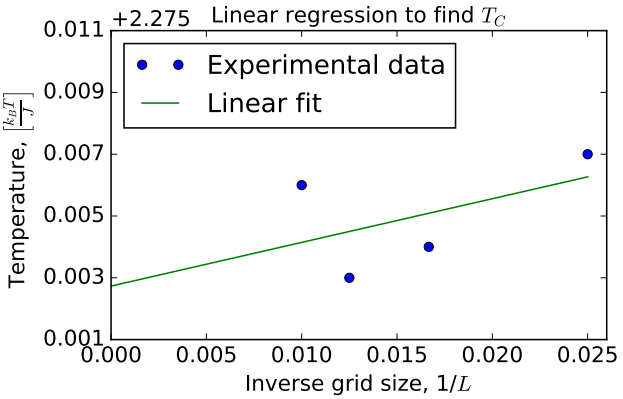


Figure 4.17: This plots show the points for $L = 40$, $L = 60$, $L = 80$ and $L = 100$ with their $T_C$s read of the plots of their temperature dependence (Figures 4.13 to 4.16). A linear regression was done on the points to find the critical temperature for $L = \infty$. The result was $T_C(\infty) = 2.278$ $k_B T/J$.

## 4.5 CPU time

The last thing we did was to see how the parallelization affected the CPU time. Table 4.2 shows the result of the timing with different number of processes. As we can read from the table, the CPU time was smaller with two processors. It was not two times faster, but that is expected due to the time used to pass messages between the processors.

Table 4.2: This is a list of the CPU time with different numbers of processes for $L$=60 and number of Monte Carlo cycles were $10^6$.

| Number of processors: | CPU time [s]: |
|---|---|
| 1 | 513.069 |
| 2 | 306.975 |

# 5 Conclusion

In this project we used a model of a magnetic material to explore different new aspects of programming. We used random number generators, the

Monte Carlo method, the Metropolis algorithm and parallelizing.

We simulated a two dimensional ferromagnetic material using the Ising model. We used Monte Carlo sampling with the Metropolis algorithm to find the steady state of the system at different temperatures and calculated the mean values of important properties of a magnetic material, the energy, the magnetic moment, the susceptibility and the heat capacity. Finally, we used these results at different temperatures to find the critical temperature where the model had a second order phase transition from ferromagnetic with a spontaneous magnetic moment, to a paramagnet with zero magnetic moment.

We made the program so that we could have run it on a supercomputer with more processors than our computers that has only two, but we chose not to do it. Running in a supercomputer with more processors than two, would have given us more data, which is important in statistical models. We also should have included unit tests in our programming, to help us during the process.

# References


[1] Morten Hjorth-Jensen. Computational physics: Lecture notes fall 2015. Department of Physics, University of Oslo, 8 2015. Chapter 2 and 6.

[2] Ising model. https://en.wikipedia.org/wiki/Ising_model. Accessed: 2017-11-17.

[3] Daniel V Schroeder. *An introduction to thermal physics*. Addison-Wesley, 2000.

[4] Full width half maximum. https://en.wikipedia.org/wiki/Full_width_at_half_maximum. Accessed: 2017-11-19.

[5] Lars Onsager. Crystal statistics. i. a two-dimensional model with an order-disorder transition. *Phys. Rev.*, 65:117–149, Feb 1944.

# Appendix

Table 5.1: This is a list of all total energy possibilities and total magnetic moment for the lattice with $L = 2$.

| State | Spin | Energy | Magnetization |
|---|---|---|---|
| 0 | ↓ ↓ ↓ ↓ | −8J | −4 |
| 1 | ↓ ↓ ↓ ↑ | 0 | −2 |
| 2 | ↓ ↓ ↑ ↓ | 0 | −2 |
| 3 | ↓ ↑ ↓ ↓ | 0 | −2 |
| 4 | ↑ ↓ ↓ ↓ | 0 | −2 |
| 5 | ↓ ↓ ↑ ↑ | 0 | 0 |
| 6 | ↓ ↑ ↓ ↑ | 0 | 0 |
| 7 | ↓ ↑ ↑ ↓ | 8J | 0 |
| 8 | ↑ ↓ ↓ ↑ | 8J | 0 |
| 9 | ↑ ↓ ↑ ↓ | 0 | 0 |
| 10 | ↑ ↑ ↓ ↓ | 0 | 0 |
| 11 | ↓ ↑ ↑ ↑ | 0 | 2 |
| 12 | ↑ ↓ ↑ ↑ | 0 | 2 |
| 13 | ↑ ↑ ↓ ↑ | 0 | 2 |
| 14 | ↑ ↑ ↑ ↓ | 0 | 2 |
| 15 | ↑ ↑ ↑ ↑ | −8J | 4 |

Table 5.2: This table lists and illustartes the possible energy changes when one spin in flipped.

| Spin configuration before | E before | Spin configuration after | E after | $\Delta E$ |
|---|---|---|---|---|
| ↑ / ↑ ↑ ↑ / ↑ | -4J | ↑ / ↑ ↓ ↑ / ↑ | 4J | 8J |
| ↑ / ↓ ↑ ↑ / ↑ | -2J | ↑ / ↓ ↓ ↑ / ↑ | 2J | 4J |
| ↑ / ↓ ↑ ↑ / ↓ | 0 | ↑ / ↓ ↓ ↑ / ↓ | 0 | 0 |
| ↓ / ↓ ↑ ↑ / ↓ | 2J | ↓ / ↓ ↓ ↑ / ↓ | -2J | -4J |
| ↓ / ↓ ↑ ↓ / ↓ | 4J | ↓ / ↓ ↓ ↓ / ↓ | -4J | -8J |